Numerical Investigation on Structural Behaviour of High Strength Cold-Formed Steel Lipped Channel Beams With V-Stiffener

Saranya.K[1], Dr. D. Amali[2]
[1]PG Student, M.E Structural Engineering, Government College of Engineering, Salem
[2]Professor, Department of Civil Engineering, Government College of Engineering, Salem

***Abstract*—Cold-formed steel (CFS) structural elements have become increasingly prominent in light-gauge construction due to their superior strength-to-weight ratio, cost-effectiveness, and design flexibility. However, their inherent thinness makes them susceptible to complex local, distortional, and global buckling phenomena. This study presents a comprehensive numerical investigation into the structural performance, load-carrying capacity, and buckling stability of high-strength steel (HSV) lipped channel beams. Utilizing the finite element software ABAQUS, non-linear numerical simulations were conducted incorporating both material and geometric non-linearities. The numerical procedure was validated against independent experimental data from literature. A detailed parametric study was executed involving 810 finite element simulations across varying cross-sectional depths, breadths, thicknesses, material types, and edge stiffener arrangements. Specifically, the nuanced influences of variations in lip length configuration (\(d/4\) and \(3d/8\)) and stiffener positioning on structural stability are analysed. The findings elucidate the critical role of edge configurations in enhancing buckling resistance and optimizing high-strength CFS elements in structural frames.**

***Index Terms*—Cold-formed steel; Lipped channel beams; High-strength variants; Finite element analysis; Local-distortional buckling interaction.**

I. INTRODUCTION

Cold-formed steel (CFS) structural components offer distinct competitive benefits over traditional hot-rolled elements, such as heightened portability, flexibility in profile configurations, and stringent quality dimensions. Despite these advantages, thin-walled CFS members face unique engineering challenges because their structural capacity is frequently limited by elastic instabilities rather than pure material yielding. When traditional hat, Z, or C-sections are subjected to compressive or bending stress below their yield strength, they undergo local (LB), distortional (DB), or global buckling (GB).

The integration of an edge stiffener, such as a lip, acts as a critical strategic mechanism to increase sectional effectiveness, delay local plate-like deformations, and significantly boost the critical moment before failure occurs. While modifying the nominal lip size affects cross-sectional efficiency, managing lip stability remains an intricate parameter during roll-forming manufacturing. Modern light-gauge building designs are increasingly incorporating high-strength variants (HSV) of steel—ranging from S700 to S1100 MPa—to capture higher strength-to-weight benefits. However, high-strength steels often exhibit a ductility trade-off that requires careful assessment, particularly under complex loading interactions such as local-distortional-global (LDG) buckling.

Understanding these complex instability phenomena under flexural conditions is vital for structural safety. Prior investigations have sought to isolate individual failure modes or assess continuous beams under non-uniform bending using the Direct Strength Method (DSM) or Effective Width Method (EWM). For instance, Zhang et al. explored the flexural responses of press-braked S690 steel channel beams under minor axis bending. Anbarasu investigated local-distortional interaction modes, while Basaglia and Camotim applied generalized beam theory and shell finite-element formulations to multi-span structures. Yu and Schafer restricted competing modes to evaluate local buckling design expressions. Nevertheless, a clear research gap remains regarding the extensive interplay between specific inside geometric configurations, lip dimensions, and stiffener positions across high-strength steel arrays. The objective of this study is to execute an automated parametric numerical analysis to optimize high-strength CFS lipped channel profiles and evaluate their capacity changes under diverse boundary arrangements.

II. LITERATURE REVIEW

Experimental and numerical studies of press-braked S690 high strength steel channel section beams.
Lulu Zhang, Fangying Wang, Yating Liang, Ou Zhao
This paper details an experimental and numerical investigation into the flexural responses and strengths of press-braked S690 high strength steel channel beams subjected to minor principal axis bending. Experimental tests included material coupon tests, imperfection measurements, and four-point bending tests, which were then used to validate finite element models. The study found that Eurocode slenderness limits could be extended to S690 steel and noted that current design codes were generally conservative but varied in precision for different slenderness levels. The authors highlighted the need for efficient design rules for high strength steels.

Local-distortional buckling interaction on cold-formed steel lipped channel beams.
Anbarasu, M. "Local-distortional buckling interaction on cold-formed steel lipped channel beams." Thin-Walled Structures 98 (2016): 351-
This paper investigates the ultimate strength and post-buckling behavior of cold-formed steel lipped channel beams under local- distortional buckling interaction. Using GBTUL-2.0β, CUFSM, and ABAQUS, the study analyzed beams with nearly equal local and distortional critical buckling stresses. A numerical parametric study was conducted, and the results were compared with existing experimental data and the Direct Strength Method (DSM). The paper proposed a design equation for such sections, highlighting the scarcity of previous research on strong local-distortional interaction effects.

Buckling, Postbuckling, Strength, and DSM Design of Cold-Formed Steel Continuous Lipped Channel Beams
*Basaglia, Cilmar, and Dinar Camotim. "Buckling, postbuckling, strength, and DSM design of cold-formed steel continuous lipped channel beams." Journal of structural Engineering 139.5 (2013): 657-*668.
This paper is part of an ongoing numerical investigation into the buckling, post-buckling, strength, and collapse behavior of cold-formed steel continuous beams. Focusing on two- and three-span lipped channel beams under non-uniform bending, the study utilized generalized beam theory and shell finite-element models.

The ultimate strength values obtained from geometrically and materially nonlinear shell finite-element analyses were compared with estimates from the Direct Strength Method (DSM) equations. The research aims to identify necessary features for a DSM approach applicable to continuous cold-formed steel beams.

Local Buckling Tests on Cold-Formed Steel Beams
Yu, Cheng, and Benjamin W. Schafer. "Local buckling tests on cold- formed steel beams." Journal of structural engineering 129.12 (2003): 1596-1606.
This research presents flexural tests on C and Z cold-formed steel sections designed to isolate local buckling by restricting distortional and lateral-torsional modes.

The study systematically varied web slenderness and other non-dimensional parameters to evaluate existing design expressions.
While overall test-to-predicted ratios were adequate, inconsistencies were noted in AISI and Canadian Standards Association (S136) provisions. The paper also pointed out that previous tests were often insufficient due to incomplete restriction of distortional mode

III. CROSS-SECTIONAL GEOMETRY AND DESIGNATIONS

The cold-formed lipped channel profile evaluated in this study features specific variations in web height (\(h\)), flange width (\(b\)), thickness (\(t\)), and downturned edge lip lengths (\(d\)) configured at fractions of \(d/4\) and \(3d/8\). To systematically establish structural performance criteria, the chosen section profiles incorporate various web-to-lip aspect ratios based on European standards (EN 10219-2:2006).

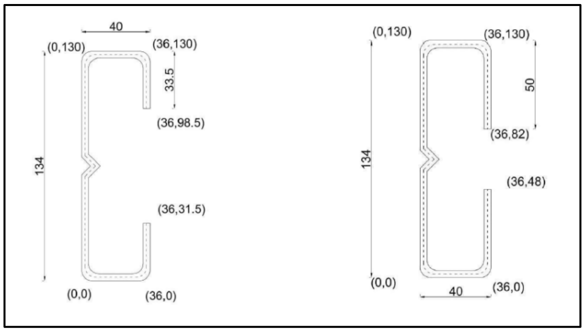

Fig. 2.1: Channel Section

The geometric matrix consists of cross-sections with flange breadths categorized at 30 mm, 40 mm, and 50 mm, combined with thicknesses of 4 mm, 5 mm, and 6 mm.

Total section depth variations (\(h\)) scale linearly alongside aspect ratios spanning from 1.00 to 2.00. Within this framework, high-strength variants (HSV) are examined across multiple web stiffener series configurations, designated as WSM (web stiffener middle), WST (web stiffener top), and WSB (web stiffener bottom) to study the spatial influence of geometric alterations on structural capacity.

TABLE-2.1 geometric details of sections

High strength variants	Placement of stiffener	h (mm)	Aspect ratio	b (mm)	t(mm)	d/4	3d/8
HSV	WSM, WST, WSB	94,102,110	1.00	30	4,5,6	24,26,28	35,39,41
		109,117,125	1.25			27,29,31	41,44,47
		124,132,140	1.50			31,33,35	47,50,53
		139,147,155	1.75			35,37,39	53,55,58
		154,162,170	2.00			39,41,43	58,61,64
HSV	WSM, WST, WSB	114,122,130	1.00	40	4,5,6	29,31,33	43,46,49
		134,142,150	1.25			34,36,38	50,53,56
		154,162,170	1.50			39,41,43	58,61,64
		174,182,190	1.75			44,46,48	65,68,71
		194,202,210	2.00			49,51,53	73,76,79
HSV	WSM, WST, WSB	134,142,150	1.00	50	4,5,6	34,36,38	50,53,56
		159,167,175	1.25			40,42,44	60,63,66
		184,192,200	1.50			46,48,50	69,72,75
		209,217,225	1.75			53,54,56	78,81,84
		234,242,250	2.00			59,61,63	88,91,94

IV. FINITE ELEMENT MODELLING AND SIMULATION

Numerical simulations were carried out utilizing the finite element (FE) suite ABAQUS/Standard to account for geometric, material, and boundary condition non-linearities. The cross-sections were modelled based on their centreline dimensions along the mid-surface plate thickness.

To discretize the shell geometries, the S4R element—a 4-noded doubly curved shell element featuring reduced integration with three translational and three rotational degrees of freedom per node—was chosen from the ABAQUS library. To ensure structural curvatures were captured with precision, corner configurations were refined using a mesh density of three specialized elements. The default longitudinal mesh layout was designated to maintain an element size equal to the section thickness, balancing simulation convergence and accuracy.

Material non-linearity was defined using a two-stage stress-strain relationship modelled via Ramberg-Osgood parameters. The initial elastic portion was defined up to the proportional limit using measured Young's modulus properties and a Poisson's ratio of 0.3, while residual stresses were omitted due to their minor impact on peak carrying capacities.

The boundary setup utilized reference points (RP1 and RP2) established at the geometric centroids of the beam ends. Rigid body and surface coupling constraints were configured to transfer force interactions effectively.
Pin-ended, simply supported support settings were applied by constraining translations across the \(x\), \(y\), and \(z\) vectors alongside designated rotational constraints.

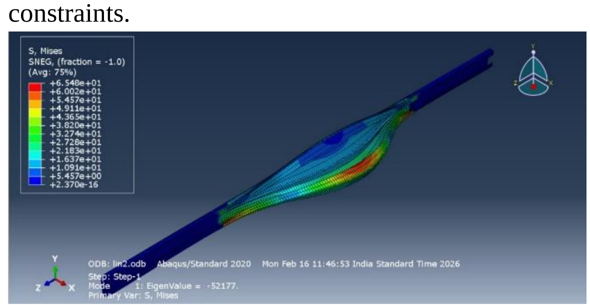

FIG-3.1 LINEAR ANALYSIS

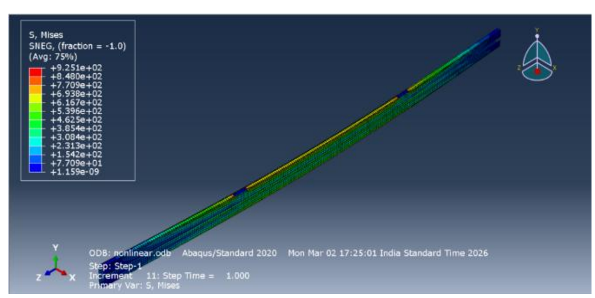

FIG-3.2 NON- LINEAR ANALYSIS

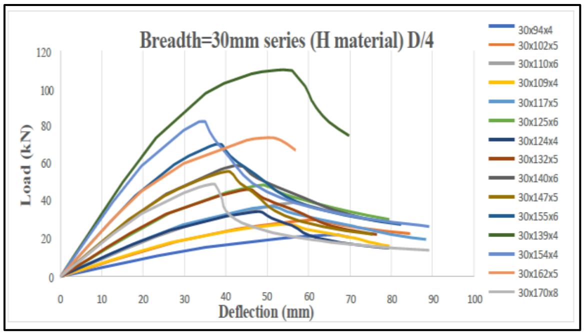

FIG-3.3 Load- deflection plot for H-30 series D/4 ratio

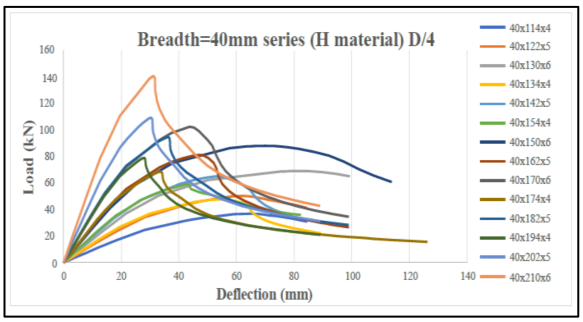

FIG-3.4 Load- deflection plot for H-40 series D/4 ratio

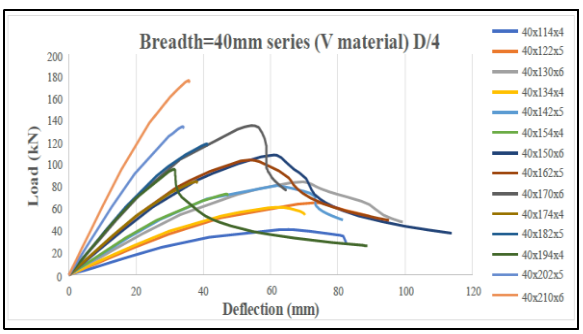

FIG-3.5 Load- deflection plot for V-40 series D/4 ratio

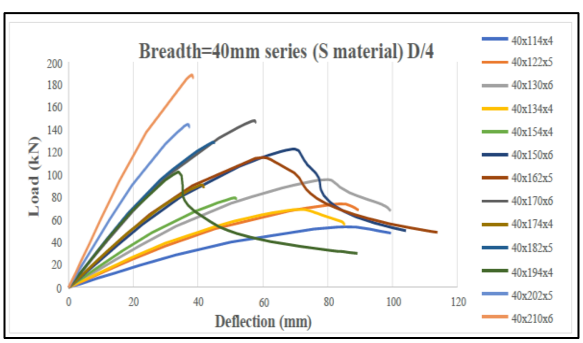

FIG-3.6 Load- deflection plot for S-40 series D/4 ratio

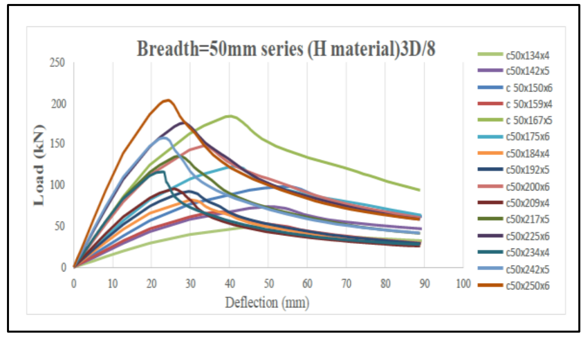

FIG-3.7 Load- deflection plot for H-50 series 3D/8 ratio

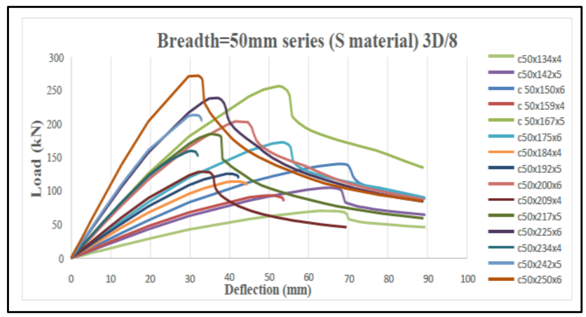

FIG-3.8 Load- deflection plot for S-50 series 3D/8 ratio

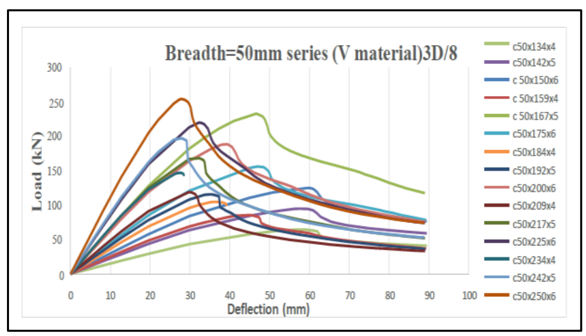

FIG-3.9 Load- deflection plot for V-50 series 3D/8 ratio

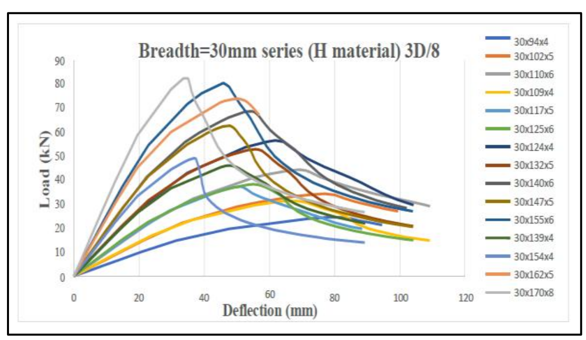

FIG-3.10 Load- deflection plot for H-30 series 3D/8 ratio

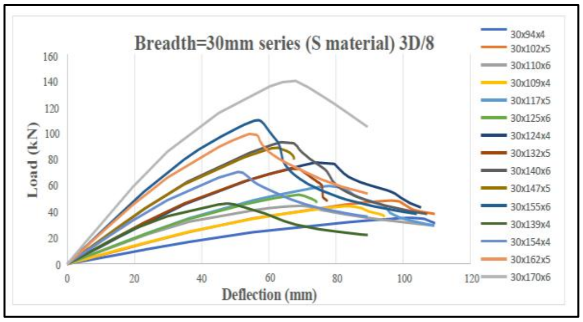

FIG-3.11 Load- deflection plot for S-30 series 3D/8 ratio

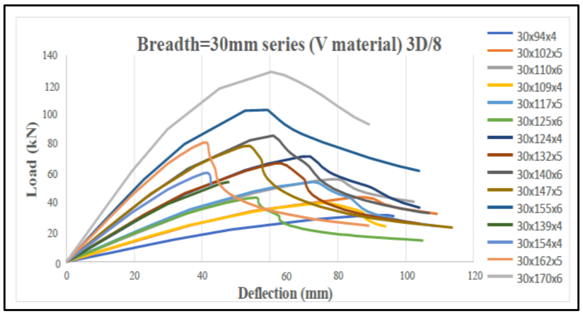

FIG-3.12 Load- deflection plot for V-30 series 3D/8 ratio

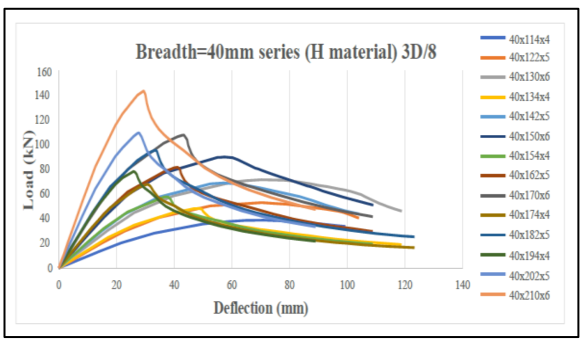

FIG-3.13 Load- deflection plot for H-40 series 3D/8 ratio

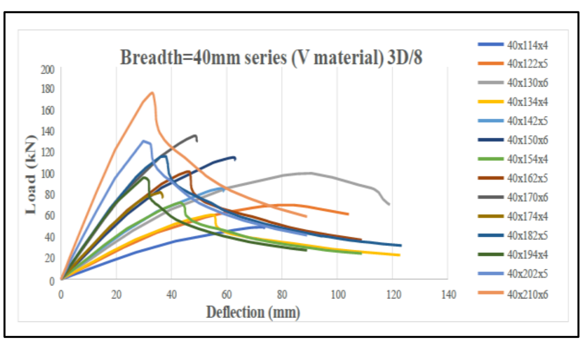

FIG-3.14 Load- deflection plot for V-40 series 3D/8 ratio

The structural solution process follows a two-tiered protocol:

1. A linear eigenvalue buckling analysis is performed under a unit load condition to establish the critical elastic buckling load values and identify the respective deformed mode profiles.
2. The extracted elastic local or global geometric mode shapes are introduced back into the system configuration as geometric initial imperfections with an amplitude of 0.1. A non-linear post-buckling solution path is then executed utilizing the arc-length solver (Static, Riks) to determine ultimate failure limits, moment capacities, and load-deformation behavioural patterns.

V. VALIDATION OF THE NUMERICAL PROCEDURE

To verify the fidelity of the finite element models, the numerical methodology was validated against the physical four-point flexural benchmarks and experimental coupon results recorded by Zhang, Wang, Liang, and Zhao. The validation models featured channel IDs such as C \(60\times40\times5\)-n, C \(80\times50\times5\)-n, and C \(100\times60\times5\)-n with flat coupon moduli near 208–212 GPa. The ultimate moment capacity values and non-linear moment-rotation patterns derived from the ABAQUS simulations showed strong agreement with the published experimental responses, confirming that the shell element mesh density, initial imperfection modelling, and solver configurations are suitable for broader parametric exploration.

VI. PARAMETRIC INVESTIGATION AND DISCUSSION

A massive sequence of 810 non-linear finite element models was executed to study the structural behaviour of high-strength cold-formed steel lipped channels. The parametric variables focused on section properties under a constant shear span of 0.7 meters, analysing performance variations between \(d/4\) and \(3d/8\) lip configuration limits.

The evaluated cross-sectional capacities emphasize the performance enhancements gained by optimization:

- In the H-WSM C(\(30\times94\times4\)) section, expanding the nominal lip dimension from 24 mm (\(d/4\)) to 35 mm (\(3d/8\)) increased the peak load from 22.19 kN to 24.57 kN, raising the ultimate moment capacity from 15.53 kNm to 17.20 kNm.
- The stiffener placement sequence also showed substantial performance deltas. The symmetric web-stiffened middle configuration (S-WSM) reached a peak moment of 21.31 kNm at \(d/4=24\) mm, which rose to 24.71 kNm under the expanded \(3d/8=35\) mm configuration.
- Thicker configurations demonstrated clear strength scaling; for instance, the S-WSM C(\(30\times110\times6\)) model reached a peak load of 52.67 kN (36.87 kNm) at a 28 mm lip size, increasing to 60.26 kN (44.23 kNm) at a 41 mm lip length.

These trends remain consistent as web height and flange thickness scale up. Profile sets such as C(\(30\times139\times4\)) and C(\(30\times155\times6\)) highlight how lengthening the lip stiffener delays the onset of distortional buckling and plate-edge bowing, enabling the high-strength steel sections to utilize more of their material capacity prior to structural failure.

VII. CONCLUSIONS

This study provided an extensive numerical exploration of high-strength cold-formed steel lipped channel beams using non-linear finite element simulations. The conclusions are summarized as follows:

1. Longitudinally configured edge lips significantly delay local and distortional buckling modes, allowing thin-walled channels to carry higher peak loads and ultimate moments before failure.
2. Increasing the nominal edge lip size from the \(d/4\) baseline to the optimized \(3d/8\) parameter increases load-carrying and structural moment capacities across all evaluated breadth and thickness profiles.
3. The positioning of web stiffeners plays a key role in stability. Symmetric double-web stiffener layouts (S-series) consistently provide superior peak capacities compared to top or bottom singular configurations under flexural demands.
4. The validated finite element methodology offers an efficient, high-accuracy alternative to expensive physical testing for optimizing cold-formed structural members.

REFERENCES

[1] AISI, *North American Specification for the Design of Cold-Formed Steel Structural Members*, AISI S100, Washington, DC, USA: American Iron and Steel Institute, 2016.

[2] Standards Australia/Standards New Zealand, Cold-Formed Steel Structures, AS/NZS 4600, Sydney, Australia: Standards Australia, 2018.

[3] European Committee for Standardization, Eurocode 3: Design of Steel Structures – Part 1-3: General Rules – Supplementary Rules for Cold-Formed Members and Sheeting, BS EN 1993-1-3, Brussels, Belgium, 2006.

[4] L. Zhang, F. Wang, Y. Liang, and O. Zhao, "Experimental and numerical studies of press-braked S690 high-strength steel channel section beams."

[5] M. Anbarasu, "Local-distortional buckling interaction on cold-formed steel lipped channel beams," Thin-Walled Structures, vol. 98, pp. 351–359, 2016.

[6] C. Basaglia and D. Camotim, "Buckling, post-buckling, strength, and DSM design of cold-formed steel continuous lipped channel beams," Journal of Structural Engineering, vol. 139, no. 5, 2013.

[7] C. Yu and B. W. Schafer, "Local buckling tests on cold-formed steel beams," Journal of Structural Engineering, vol. 129, no. 12, pp. 1596–1606, 2003.

[8] L. Laím, J. P. C. Rodrigues, and L. S. da Silva, "Experimental and numerical analysis on the structural behaviour of cold-formed steel beams," Thin-Walled Structures, vol. 72, pp. 1–13, 2013.

[9] M. A. Dar, M. Yusuf, A. R. Dar, and J. Raju, "Experimental study on innovative sections for cold-formed steel beams," Steel and Composite Structures, vol. 6, pp. 1599–1610, 2015.

[10] Y. L. Li, Y. Q. Li, and Z. Y. Shen, "Investigation on flexural strength of cold-formed thin-walled steel beams with built-up box section," Thin-Walled Structures, vol. 107, pp. 66–79, 2016.

[11] L. P. Wang and B. Young, "Behavior of cold-formed steel built-up sections with intermediate stiffeners under bending. I: Tests and numerical validation," Journal of Structural Engineering (ASCE), vol. 142, no. 3, Art. no. 04015150, 2016.

[12] L. P. Wang and B. Young, "Behavior of cold-formed steel built-up sections with intermediate stiffeners under bending. II: Parametric study and design," Journal of Structural Engineering (ASCE), vol. 142, no. 3, Art. no. 04015151, 2016.

[13] J. Ye, S. M. Mojtabaei, I. Hajirasouliha, P. Shepherd, and K. Pilakoutas, "Strength and deflection behaviour of cold-formed steel back-to-back channels," Engineering Structures, vol. 177, pp. 641–654, 2018.

[14] D. K. Phan and K. J. R. Rasmussen, "Flexural rigidity of cold-formed steel built-up members," Thin-Walled Structures, vol. 140, pp. 438–449, 2019.

[15] M. A. Dar, N. Subramanian, A. R. Dar, M. Lim, M. Anbarasu, J. B. P. Lim, and A. Mir, "Behaviour of partly stiffened cold-formed steel built-up beams: Experimental investigation and numerical validation," Advances in Structural Engineering, vol. 22, no. 1, pp. 172–186, 2019.

[16] M. Anbarasu, "Simulation of flexural behaviour and design of cold-formed steel closed built-up beams composed of two sigma sections for local buckling," *Engineering Structures*, vol. 191, pp. 549–562, 2019.